

Property Predictions for Packed Columns Using Monte Carlo and Discrete Element Digital Packing Algorithms

C. Xu¹, X. Jia², R. A. Williams², E. H. Stitt³, M. Nijemeisland³, S. El-Bachir⁴
A. J. Sederman⁴ and L. F. Gladden⁴

Abstract: Existing theories and computer models for packed columns are either incapable of handling complex pellet shapes or based on oversimplified packing geometry. A digital packing algorithm, namely DigiPac, has recently been developed to fill the gap. It is capable of packing of particles of any shapes and sizes in a container of arbitrary geometry, and is a first step towards a practical computational tool for reliable predictions of packed column properties based on the actual pellet shapes. DigiPac can operate in two modes: a Monte Carlo mode in which particles undergo directional diffusive motions; and a Discrete Element mode where translations and rotations of particles are governed by physical laws. The former is faster but in certain cases less accurate, whereas the latter is slower but produces significantly more accurate predictions. Both modes have been used in simulating packed columns of real pellet shapes. Results for cylinders – one of the most commonly used shapes for packed columns – are reported. Comparisons are made between DigiPac predictions under different modes and experimental data obtained using nuclear magnetic resonance (NMR) imaging technique. Good agreement between simulation and NMR results has been observed.

Keyword: Packed Column, Particle Packing, Property Prediction, Digital Packing Algorithm, Discrete Element Method.

1 Introduction

Packed columns are common devices frequently encountered in many areas of chemical engineering industry which deal with mass transfer operations, such as petroleum refining, petrochemical, pharmaceutical, food processing and environmental processing. These applications in general include the functions of absorbing, stripping, distillation, separation or extraction. The performances with regard to these operational functions directly quantify the effectiveness and efficiency of the packed column. It is generally agreed that these performances depend heavily on the column structure, which in turn depends on the column geometry and, most importantly, the pellets used and how they are packed to form the bed. The success of the operation is, therefore, boiled down to a design issue where it is vital to be able to relate the performances to the pellet geometry and the packing method directly and inexpensively.

Detailed structural characteristics inside the columns such as local voidage, accessible areas and void uniformity are generally considered the main factors affecting the effectiveness and efficiency of the packed bed. Ironically these factors are not considered directly in the current design practice, with the major obstacle being the lack of a reliable tool which can predict the internal detailed packing structure for pellets and columns of practical complexity. As a result, the current practice relies either on historical empirical correlations, if the geometry of the pellets and the column and the type of applications are covered by these correlations; or on a trial-and-error approach based on expensive physical experiments, if not [Strigle, 1994]. In either of these practices, the column structures are treated as “black

¹ School of Civil, Environmental and Mining Engineering, University of Adelaide, Australia.

² Institute of Particle Science and Engineering, School of Process, Environmental and Materials Engineering, University of Leeds, Leeds LS2 9JT, UK.

³ Johnson Matthey Catalysts, Cleveland TS23 1LB, UK.

⁴ Department of Chemical Engineering, University of Cambridge, Pembroke Street, Cambridge CB2 3RA, UK.

boxes” and only input-output relations are established and the detailed process inside the column is normally not part of the equation.

A digital packing algorithm, namely DigiPac, has recently been developed to fill the gap. It is capable of packing of particles of any shapes and sizes in a container of arbitrary geometry, and is a first step towards a practical computational tool for reliable predictions of detailed packed column properties based on the actual pellet shapes. The technique has been successfully applied recently in various projects [Gan, Gopinathan, Jia and Williams (2004); Jia, Gan, Williams and Rhodes (2005)]. DigiPac can operate in two modes: Monte Carlo mode (MC packing) and Discrete Element mode (DEM packing), and the suitability of the mode in practice will be application dependent. In Monte Carlo mode, particles undergo directional diffusive motions assigned randomly and no physical interactions between particles are considered and therefore it is more likely to produce loose packing structures in some cases. In Discrete Element Modelling mode particle translations and rotations of particles are governed by physical laws and therefore denser packing structures can be achieved.

MC packing case studies involving mono sized spheres and binary and ternary mixtures of spheres have already been reported elsewhere [Caulkin, Fairweather, Jia and Williams (2006)] and will not be repeated here. In the case study reported here, a column is packed with short cylinder pellets using both MC and DEM modes and its packing density and spatial statistical characteristics are compared with an experimental dataset acquired by magnetic resonance imaging (NMR). As expected, MC packing mode of the digital algorithm produces lower packing density while the DEM mode produces results much closer to that of the NMR dataset. The structure of the NMR dataset is believed to be a random dense packing structure due to vigorous taping used in the packing process.

2 The digital packing algorithms

The term “digital packing” here specifically refers to the fact that in the world of digital pack-

ing everything involved is digitized, meaning in this case that column geometry and all particles are represented by voxels in 3D or pixels in 2D during the packing process. Thus any physical shape is simply a coherent collection of voxels, which resides and moves in a 3D (2D) lattice grid representing digitally the space in which particles pack [Jia and Williams (2001); Gopinathan, Fairweather and Jia (2003)]. This is in contrast to conventional approaches where objects are in general represented by polygons approximating the surface embracing the objects, except for some simple geometrical cases where an accurate mathematical description is possible, e.g., spheres, cubes. In packing simulations, the polygonal surface approach is obviously limited in its usefulness in practice. The two main drawbacks include the facts that large numbers of polygons are required to represent even a geometrical shape with moderate complexity (e.g., an apple), and equally seriously, it is technically difficult to derive a general implementation for the contact and overlap detections between particles of any shapes with certain degree of complexity. As a result, available commercial packing software [e.g., MacroPac, SperoPolyhedra] can only deal with simple geometrical shapes such as spheres or shapes that can be reasonably approximated by spheres. In the academic community, a few in-house packing programs [Dickinson and Knopf (1998); Kohlus and Bottlinger (1998)] known to us not only demand super computing power but also are limited to handle small number of complex shapes. Munjiza and Andrew (1998) has introduced computational solutions such as NBS, distributed contact force approach for real shaped particles and finite rotation solver, which enable large number of particles to be considered on a PC. However, these algorithms are much more complex and more difficult to implement than the digital packing to be described.

The digital packing approach, however, overcomes these problems in a simple manner. The number of voxels required to represent an object does not depend on the complexity of the shape of the object. Detections of contacts and overlaps between particles become a simple matter of

checking if two voxels, each from a different object, are adjacent or occupying the same site on the lattice grid. No complicated geometrical operations are involved. The digitization of particles does not impose serious overhead either. In fact, pallets for most packed column applications are usually designed in a CAD system using a format that can be easily converted into digital representations. For applications (e.g., high-performance liquid chromatography) involving small powder particles ($< 2\text{cm}$) where the CAD data is not available, the digitization of particles can be derived from x-ray micro tomography (XMT) images, confocal microscopy, optical profilometry or Scanning Electron Microscope/Transmission Electron Microscope (SEM/TEM) images.

As in all digitization process, however, there is also an issue of digitization error in the digital representation of particles. In digital packing algorithms, this error can be quantified by surface and volume representation errors (i.e., the relative differences in surface area and volume between the true and the digital representation), which are directly related to the scale used and that in turn will affect the accuracy of the final packing structure. The two error terms are related. The volume representation error, however, is more relevant to packing applications as packing density in general is the major interest of the investigation in these applications. The surface area representation error only becomes important for property (e.g., flow) analysis of the packed structure where a surface smoothing process can be applied to reduce the effect of the error. Detailed discussion of the surface smoothing is beyond the scope of this paper.

The size of a voxel in the digital representation can be mapped into different physical sizes and therefore different scales of representations of the objects can be created. For example, Figure 1 shows a sphere of physical diameter of 50 mm and two digital representation using 50 voxels diameter (hence the scale of $s = 1\text{ mm/voxel}$) and 100 voxels diameter (hence the smaller scale of $s = 0.5\text{ mm/voxel}$). It is in general expected that the volume digitization errors will diminish as the scale decreases, implying more accurate representation,

see the example error curves for spherical objects shown in Figure 2 (Note surface representation error will not disappear but stabilizes at the value of 50%, which is the inherent surface error term of the digital representation for spheres). There is, however, a penalty for using smaller scale as the computing time involved for packing the particle will increase roughly with $(1/s)^3$. In practice, a compromise is usually needed between the accuracy requirement and the time scale desired or the computing resource available.



(a) Sphere ($D = 50\text{ mm}$) (b) Digital sphere ($s=1$) (c) Digital sphere ($s=0.5$)

Figure 1: Sphere of diameter 50 mm and its two digital representations

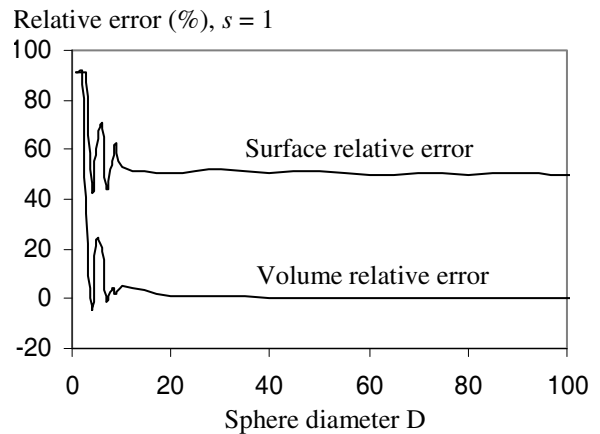


Figure 2: Digital representation errors for spheres

2.1 Monte Carlo packing

In this mode, all particles are subjected to random translations and rotations during the settling process. The translation direction and rotation parameters are generated using the Monte Carlo method. Uniform distributions are in general used in the MC sampling process, implying equal

chance of selection for different translation directions and different rotation parameters. The upward movement is, however, only accepted with a so-called rebounding probability (< 1.0) to ensure particles the general trend of settling downward. The use of rebounding probability effectively increase the chance for particles to move out of local stabilization (e.g., particles inter-locking locally) towards global stabilization, similar to the role played by the annealing probability used in simulated annealing and the acceptance probability used in the Markov-Chain Monte Carlo (MCMC) process. The use of random rotations helps particles to explore all possible packing space and in general no restriction is imposed on the generated parameters. A more detailed account of the Monte Carlo digital packing algorithm can be found in Jia and Williams (2001).

Monte Carlo digital packing is purely stochastic, no physical interactions between particles are considered. Movement of a particle is simply discarded if it causes overlaps with other particles or the container. This lack of physical law guidance makes the Monte Carlo packing difficult, though statistically possible, to converge to a very dense packing structure. As a result, the packing structure achieved after certain number of iterations is only one possible stable structure between the random loose and dense structures.

2.2 DEM packing

DEM digital packing, on the other hand, imposes the physical interactions between particles in the form of DEM on top of digital packing algorithm. Particle translations and rotations are no longer random but governed by the contact and gravitational forces acted on the particles during the settling process. In this case, small amount of overlap between particles is allowed to simulate deformations when particles come into contact with each other and these deformations are then used to calculate contact forces between particles. There is a fundamental difference between digital DEM used here and the conventional DEM. In conventional DEM, deformations are considered at the particle level while in digital DEM they are at voxel level. Contact forces acting on a particle

are derived by summing up the individual contact force components acting on the surface voxels of the particles (note the summing here is not a simple arithmetic summing process, number of contacts between particles should also be considered). Such a treatment in digital DEM in fact simplifies a great deal the force calculations as the directions of forces acting at the voxel level are always orthogonal and coincide with the lattice grid system.

There is no shortage of publications about conventional DEM algorithm [Cundall and Strack (1979); Munjiza (2004); Jing and Stephansson (2004)]. The basic spring dash-pot model is used in digital DEM but at the voxel level. A 2D example is shown in Figure 3, illustrating models needed for a protruding surface pixel. For each out-facing face of the pixel, the normal and tangential forces are calculated as:

$$F_{n,t} = (-k_{n,t}\delta_{n,t} - \eta_{n,t}v_{n,t})\bar{n}_{n,t} \quad (1)$$

Where $k_{n,t}$, $\delta_{n,t}$, $\eta_{n,t}$ and $v_{n,t}$ are the stiffness, overlap, dumping coefficient and relative velocity component in normal (\bar{n}_n) and tangential (\bar{n}_t) directions respectively.

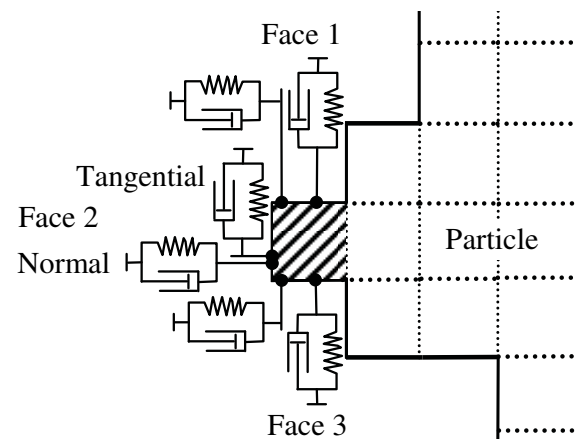


Figure 3: Contact force models in digital DEM

To sum up, the following steps will be needed to establish the kinematics and movements of a particle at a particular time step:

- Loop over all the surface voxels of the particle, find the contacted voxels from other par-

ticles and evaluate the contact forces based on the overlap values (see above).

- Calculate the translation forces for the particle by summing up the surface voxel contact forces in the three major directions in the lattice grid system.
- Calculate the total torque acting on the particle against the centre of gravity of the particle and around the three major axes of the lattice grid system by summing up the torque created by contact forces of individual surface voxels.
- Establish the new translational and rotational movements for the particle (accelerations and speeds) based on Newtonian laws.
- Update the locations and orientations of the particles according to the new translational and rotational speeds calculated at this time step.

2.3 NMR data set

The bed of cylinders consisted of porous alumina particles with a diameter of 5.40 ± 0.05 mm and a length of 3.80 ± 0.20 mm packed into a 70 cm long nylon column with a diameter of 43.3 ± 0.1 mm. The column was sealed at the ends with screw caps. The porous cylinders were submerged in water before packing to ensure liquid saturation. Great care was taken in the packing of the cylinders to prevent bridging of particles and to ensure as homogeneous a packing structure as possible. The bed of cylinders was packed using a UNIDENSE™ tool. To avoid air bubble entrapment within the packing, the column was filled with water progressively as particles were loaded such that the top of the bed was always submerged by at least 10 cm. The UNIDENSE™ tool was first inserted into the column. Then the packing particles were poured continuously into the column. When the column was filled the packing was consolidated by tapping on the external column wall. As the column was tapped the height of the bed decreased as the void space was reduced; fresh particles were added to the top of the bed as required. The tapping ceased

after no further compaction was possible. At the end the bed was fully submerged in water.

2.4 MRI

The column packed with cylinders was placed vertically inside the magnet bore. ^1H MRI data were acquired at a frequency of 199.7 MHz on a Bruker Spectrospin DMX 200, 4.7 T magnet with a birdcage coil of diameter 6.3 cm and shielded gradient coils providing a maximum gradient strength of 13.5 G cm^{-1} . A high spatial resolution image of the bed was acquired using a 3D-RARE pulse sequence [Henig, Nauerth and Friedburg (1986)]. A resolution of $180\mu\text{m} \times 180\mu\text{m} \times 180\mu\text{m}$ was obtained for a matrix of $256 \times 256 \times 512$ voxels and a field-of-view of $46 \text{ mm} \times 46 \text{ mm} \times 92 \text{ mm}$ with the higher field-of-view in the axial direction. The axial extent of the imaging coil was approximately 45 mm and the imaging region was close to the centre of the column to avoid packing effects from the top and bottom. A recycle time of 5s, an echo time of 6.9ms, 4 averages and a RARE factor of 32 were used giving a total acquisition time of 11.5 h and effective echo time of 117ms. An advantage of the RARE image sequence is that it is T_2 -weighted with a large effective echo time. In this system the inter-particle water has a T_2 of $\sim 500\text{ms}$ and is therefore observed in the image but the intra-particle water, which has a very short T_2 of $\sim 7\text{ms}$, is not seen in the image providing excellent contrast between inter- and intra-particle water. This allows us to differentiate between the voxels corresponding to packing elements, those with a lower signal intensity as a result from the short (intra-particle) T_2 , and those with a high signal intensity corresponding to the void space. For an introduction to the principles of MR techniques, the reader is referred to excellent texts by Callaghan (1991) and Kimmich (1997).

3 Packing density

The voidage and the distributions of voids directly affect the effectiveness and efficiency of the packed column. Therefore voidage (hence packing density) is in general the most studied parameter to be related to the performances in packed

column applications. It is also the parameter that can be easily measured to a certain degree of accuracy in a controlled experimental environment. As the first comparison, we compare the packing densities of the packing structures obtained by experiment (NMR), Monte Carlo DigiPac and DEM DigiPac simulations. For a randomly packed structure (by experiment, Monte Carlo or DEM method), average cross-sectional densities (cross-sections perpendicular to column axis), i.e., the axial densities, are expected to vary randomly along the column axis, except at the top and bottom of the column where wall effects dominate and introduce distortions in the density profile. Figure 4 shows the density profiles of the structures together with their statistical distributions. For each type of packing (MC and DEM), a total of three simulations were run.

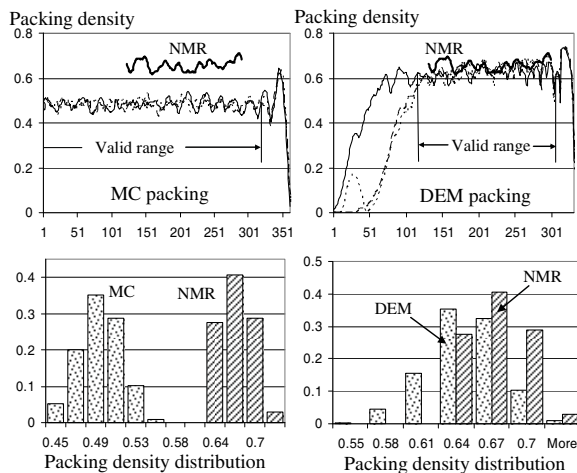


Figure 4: Axial packing density along the column axis

Normal distributions are observed in all cases, implying random packing structures in all three cases. The mean (m) and standard deviations (σ) of the distributions are summarized in Table 1. The closeness of the standard deviations of the three cases confirms the correctness of the simulation setups. The mean packing density by MC simulation is 26% lower than that of the NMR data, while the DEM packing achieves a mean packing density which is only 4% lower. These figures support the suggestions that MC digital

packing generates packing structure closer to random loose packing and DEM digital packing generates structure closer to random dense packing. These claims are also evident by the visual inspection of the examples of packing structures shown in Figure 5. The “gaps” between pallets in the MC packed structure are obviously greater than those shown in the other two structures.

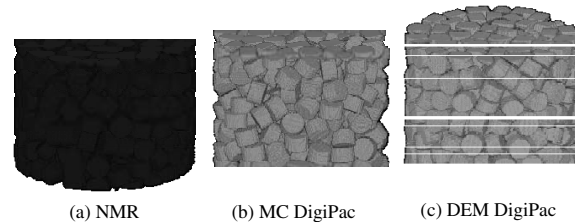


Figure 5: Examples of packing structures of the three cases

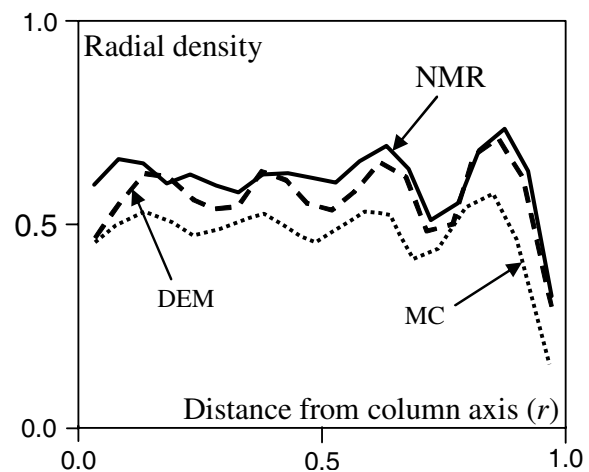


Figure 6: Comparison of radial density profiles

The digital packing structures generated by DigiPac simulations can easily be used for further analysis of the structural properties, such as local voidage, void distributions, coordination numbers or pallet orientations, which in general are difficult to measure by experiment. We here present, in Figure 6, the comparison of the radial density profiles (averaged values over the simulations) of the structures. The voidage distribution along the column radius is also an important property affecting the performance of the packed column.

Two observations can be made. First, the trends of radial density profiles obtained by MC and DEM simulations both follow qualitatively that of the NRM data, with the DEM profile follows more closely. They all express cyclic damping variations towards the column axis, suggesting layered pallet structures starting at the column wall, see the shadow images of the three cases shown Figure 7. The reduction in the density variation closer to the column axis implies that the layered pallet structure becomes less dominant and the structure tends towards more uniform. Secondly, there is a less erratic appearance in the variation of the MC simulation density profile, which suggests that the structure generated by MC simulation is more uniform, implying the structure is more loosely and uniformly packed (see also **Figure 7**). This point is also evident by comparing the standard deviations listed in **Table 1**.

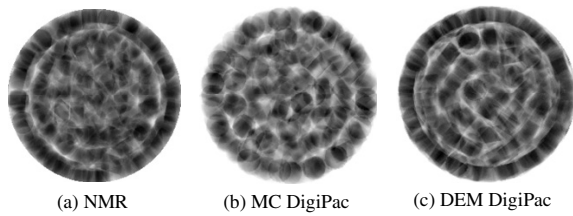


Figure 7: Shadow images of the packing structures for the three cases

Table 1: Statistics of packing density for the three cases

	NMR	MC digital packing	DEM digital packing
Mean (m)	0.657	0.484	0.634
Standard deviation (σ)	0.022	0.020	0.030

4 Spatial statistics

As a way to quantify the void distributions inside the column, the spatial void correlation functions are further investigated. We first define an indica-

tor variable, $I(x)$ as:

$$I(x) = \begin{cases} 1 & \text{if the site at location } x \text{ is a void} \\ 0 & \text{otherwise} \end{cases} \quad (2)$$

where x denotes a point in space. $I(x)$ thus represents the void structures as shown in Figure 8. This variable is used to calculate spatial correlation characteristics for the void inside the column. The two-point probability function $S_2(h)$ defined by Torquato (2002) is used here to quantify this correlation. $S_2(h)$ is in essence the conditional probability of finding a void site of distance h away from a known void site x , with asymptotic value equal to the square of the mean porosity, i.e., the probability of finding a void site in pure random case. Figure 9 compares the $S_2(h)$ functions for the structures generated by the packing simulations and from the NMR data.

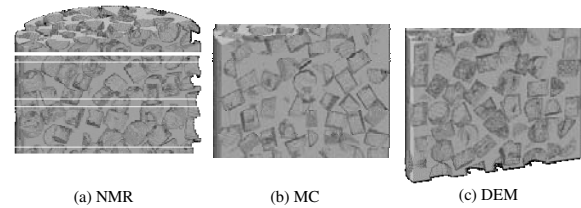


Figure 8: Examples of the void structures for the three cases

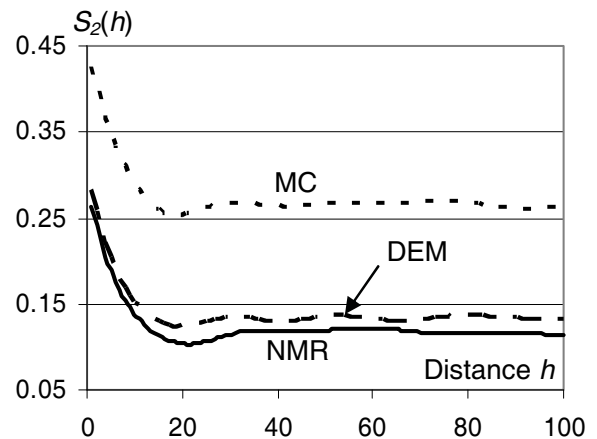


Figure 9: $S_2(h)$ functions for the three cases

As expected, $S_2(h)$ function for DEM simulation closely resembles that of the NMR data, suggesting very similar spatial statistical characteristics

between the two void structures. The shorter correlation range ($h \approx 18$) of the void structure by MC simulation compared with that of the DEM simulation or the NMR data ($h \approx 32$) indicates that the void structure by MC simulation is more randomly (or uniformly) distributed.

Mean empty space [Zeidan, Jia and Williams (2003)] is also an effective property to characterize void distributions inside the packed column. The statistics have been calculated and are presented in Figure 10. The mean empty space is calculated as the mean spacing between the solids in a void space. It is used here as a measure of the average ‘pore’ size.

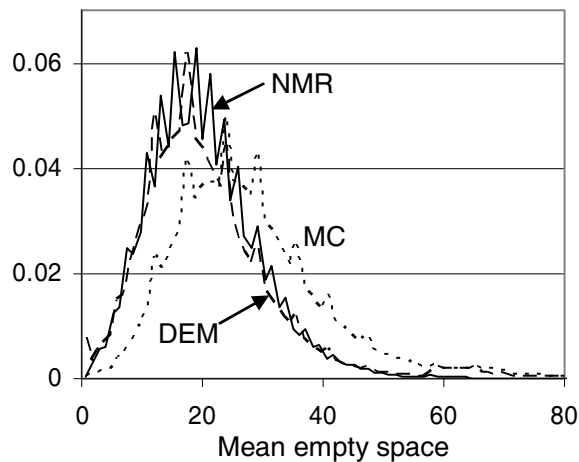


Figure 10: Mean empty space distributions

All mean empty space distributions are of lognormal type. The DEM case follows again closely the NMR data, while the MC case shifts slightly towards normal distribution, implying the void structure is spatially more uniformly distributed. Note that the mean empty space used here is fundamentally different to the pore size defined in Torquato (2002), or the first contact distance defined in Stoyan, Kendall and Mecke (1995). The later two definitions lead to the pore size distribution function [Torquato, 2002] and the spherical contact distribution function or first contact distribution function [Stoyan, Kendall and Mecke (1995)].

5 Conclusions

The following conclusions can be drawn from the results presented in this report:

1. The digital packing algorithm (DigiPac) is a simple but effective and efficient approach for particle packing simulations. The simplicity of the algorithm in particle representation, movements and contact and overlap detection does not change with the complexity of the shapes of the particles. This makes it an ideal computational method for practical applications.
2. In Monte Carlo mode, the digital packing algorithm tends to generate loose packing structures, while the DEM mode is able to produce dense packing structure.
3. Packing density and other spatial statistics reveal very similar characteristics between MC or DEM simulated structures and the NMR imaged structure. The MC packing structure is spatially more uniformly distributed, confirming that the MC packing is orientated more towards random loose packing. The DEM packing structure in this case follows very closely the NMR data set (a dense packing structure) in the statistics presented.

Further investigation will be needed to quantify the degrees of ‘closeness’ to random loose or dense packing of structures generated by digital packing algorithm (DigiPac). It will also be useful to relate the simulated structures to packed column performances (such as effectiveness, efficiency) so that the suitability of the algorithm (and the different packing modes) for practical applications can be assessed.

Acknowledgement: The work reported in this paper was funded by EPSRC (Engineering and Physical Sciences Research Council) grants EP/D503078, GR/S20789/01 and GR/R47523/01, and Johnson Matthey plc.

References

- Dickinson, J.K.; Knopf, G.K.** (1998): Generating 3D packing arrangements for layered manufacturing, Rensselaer's International Conference on Agile, Intelligent, and Computer Integrated Manufacturing, Troy, New York, Oct., 1998.
- Callaghan, P.T.** (1991): *Principles of Nuclear Magnetic Resonance Microscopy*, Clarendon, Oxford, ISBN: 0198539444.
- Caulkin, R.; Fairweather, M.; Jia, X.; Williams, R. A.** (2006): An investigation of packed columns using a digital packing algorithm, *Computers and Chemical Engineering*, vol. 30, pp. 1178-1188.
- Cundall, P.A.; Strack, O.D.L.** (1979): A distinct numerical model for granular assemblies, *Geotechnique*, 29, pp. 47-65.
- Gan M.; Gopinathan N.; Jia X.; Williams R.A.** (2004): Predicting packing characteristics of particles of arbitrary shapes. *KONA Powder and Particle*, 22:82-93.
- Gopinathan, N.; Fairweather, M.; Jia, X.** (2003): *Computational modeling of packed bed systems*, Proc. ESCAPE-13, Elsevier, Amsterdam, 647p.
- Hennig, J.; Nauerth, A.; Friedburg, H.** (1986): *Magnet. Reson. Med.* 1986, 3, pp. 823-833.
- Jia X.; Gan M.; Williams R.A.; Rhodes D.** (2005), Validation of a digital packing algorithm in predicting powder packing densities, presented at the Particulate Systems Analysis 2005, 21-23 September 2005, Stratford on Avon, UK.
- Jia, X.; Williams, R.A.** (2001): A packing algorithm for particles of arbitrary shapes, *Powder Technology*, vol. 120, pp. 175-186.
- Jing, L.; Stephansson, O.** (2004): *Fundamentals of discrete element methods for rock engineering*, Elsevier, ISBN: 0444829377.
- Kimmich, R.** (1997): *NMR Tomography, Diffusometry, Relaxometry*. Springer-Verlag, Berlin Heidelberg, ISBN: 3540618228.
- Kohlus, R.; Bottlinger, M.** (1998): Computer simulation and characterization of bulk solids built by irregularly shaped particles, in Proceedings of the 3rd World Congress on Particle Technology, Article No. 42. 7-9 July 1998, Brighton, UK.
- MacroPacTM from Intelligensys Ltd (www.intelligensys.co.uk).
- Munjiza, A.; Andrews, K.R.F.** (1998): NBS contact detection algorithm for bodies of similar size, *Int J Numer Meth Engng*, vol. 43, pp. 131-149.
- Munjiza, A.** (2004): *The combined finite-discrete element method*, John Wiley & Sons, ISBN: 0470841990.
- SpheroPolyhedraTM from Smart Image Technologies (www.simagis.com).
- Strigle, Jr, R.F.** (1994): *Packed Tower Design and Applications*, 2nd edition, Gulf Publishing Company, London. ISBN: 0884151794.
- Stoyan, D.; Kendall, W.S.; Mecke, J.** (1995): *Stochastic Geometry and Its Applications*, John Wiley & Sons, ISBN: 0471950998.
- Torquato, S.** (2001): *Random Heterogeneous Materials: Microstructure and Macroscopic Properties*: v. 16 (Interdisciplinary Applied Mathematics Series), Springer-Verlag, New York. ISBN: 0387951679.
- Zeidan, M.; Jia, X.; Williams, R.A.** (2005): Simulation of aggregation with applications to soot laden lubricating fluids, *Particle and Particle Systems Characterization*, vol. 21(6), pp. 473-482.

